Supporting Information

Almaraz, P. and Green, A.J. (2024) Catastrophic bifurcation in the dynamics of a threatened bird community triggered by a planetary-scale environmental perturbation. *Biological Conservation*. https://doi.org/10.1016/j.biocon.2024.110466

Contents

S1 Regularization of interaction coefficients in the regime-dependent LVR model

In natural communities of interacting species most of the potential inter-specific interactions are generally weak, and this is known to stabilize competitive communities [1–8]. Besides, for high-dimensional hierarchical Bayesian models, such as the state-space regime-dependent LVR model used here, it is desirable to control for potential issues with MCMC convergence and posterior cross-correlations among parameters induced by the large amount in inter-specific interactions fluctuating around 0 [4, 9–11]. To this end, we used a regularization (sparsity-inducing) scheme on the inter-specific interactions of matrix **A**, the $\alpha_{i,j}$'s. Through regularization methods those parameters whose impact on the posterior probability is weak are set to 0 during the MCMC simulation. At the same time, regularization schemes should be able to simultaneously let those interactions with significant effects on the posterior to be estimated freely. We use Stochastic Search Variable Selection (SSVS; [12]) to automatically set to 0 the inter-specific interactions with a weak effect on the posterior during the MCMC simulation. Specifically, we induced a spike-and-slab prior [13] for the distribution of the $\alpha_{i,j}$'s. Let's define the probability of inclusion of a given interaction coefficient $\alpha_{i,j}$ as a random variable p, following a discrete Bernoulli distribution,

$$p \sim \text{Bern}(\nu) \tag{S1}$$

where ν is the prior probability of inclusion of the interaction coefficient. We let this prior probability to follow a weakly informative Beta distribution to let the model learn from sparsity during the posterior simulation,

$$\nu \sim \text{beta}(2, 8) \tag{S2}$$

The $\alpha_{i,j}$'s are then modeled as:

$$\begin{aligned} \alpha_{i,j}|p = 0 &\sim \delta_0 \\ \alpha_{i,j}|p = 1 &\sim \mathcal{N}\left(0, \sigma^2_{\text{slab}}\right) \end{aligned} \tag{S3}$$

where δ_0 is the Dirac's Delta distribution at 0 (so-called 'spike'), and σ^2_{slab} is the variance of the interaction coefficient $\alpha_{i,j}$ when it is estimated freely (so-called 'slab'). We placed a large variance for the slab, $\sigma^2_{\text{slab}} = 10$. Marginalizing over p, we thus can write

$$\alpha_{i,j} = p\mathcal{N}(0, \sigma^2_{\text{slab}}) + (1 - p)\delta_0 \tag{S4}$$

In essence, this means that when the parameter p is activated (that it, when it takes a value of 1), the interaction coefficient is estimated according to the standard normal distribution with variance σ^2_{slab}, $\alpha_{i,j} \sim \mathcal{N}\left(0, \sigma^2_{\text{slab}}\right)$. In contrast, when p is deactivated (it takes a value of 0), the interaction coefficient follows a Dirac's Delta distribution

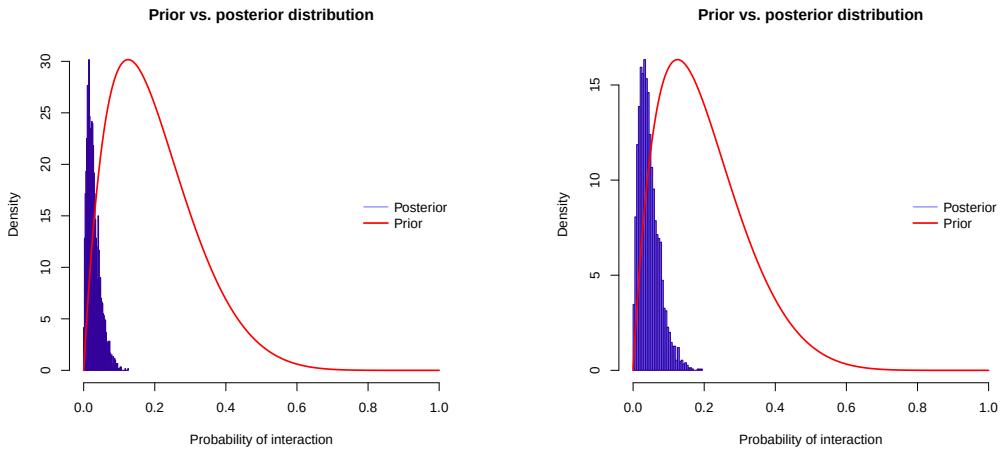

(a) **Before** the Pinatubo eruption (b) **After** the Pinatubo eruption

Figure S1: The histograms show the posterior distributions of the probability of inter-specific interactions for the regime-dependent state-space LVR model before (A) and after (B) the Mt. Pinatubo eruption. The red curves show the prior distribution of probability of interaction, represented in Eqn. S1 as $\nu \sim \text{beta}(2, 8)$.

at 0. That is, it is effectively 0 (see [13]). This means that the posterior probability of inclusion of an interaction coefficient $\alpha_{i,j}$ is the proportion of times that the parameter was active during the MCMC simulation, i.e., the number of times that $p = 1$. In Fig. S1 we represent the posterior distribution of the probability of inter-specific interaction for each regime against the prior probability (ν). Results suggests that the probability of finding strong inter-specific interactions coefficients among the wintering waterfowl community of Doñana wetlands is very low in both stable states.

S2 Impact of flooding extension on community dynamics

Figure S2 shows the posterior distribution of the impact of flooding extension on the growth rate of each waterfowl species wintering in Doñana wetlands (parameters γ_i in the LVR model of the accompanying paper). The effects are generally positive for all species in both regimes.

S3 Posterior predicted datasets

Figure S3 show the posterior predicted datasets testing the ability of the fitted state-space regime-dependent LVR model to replicate the time-series of community abundance before (A) and after (B) the Mt. Pinatubo eruption.

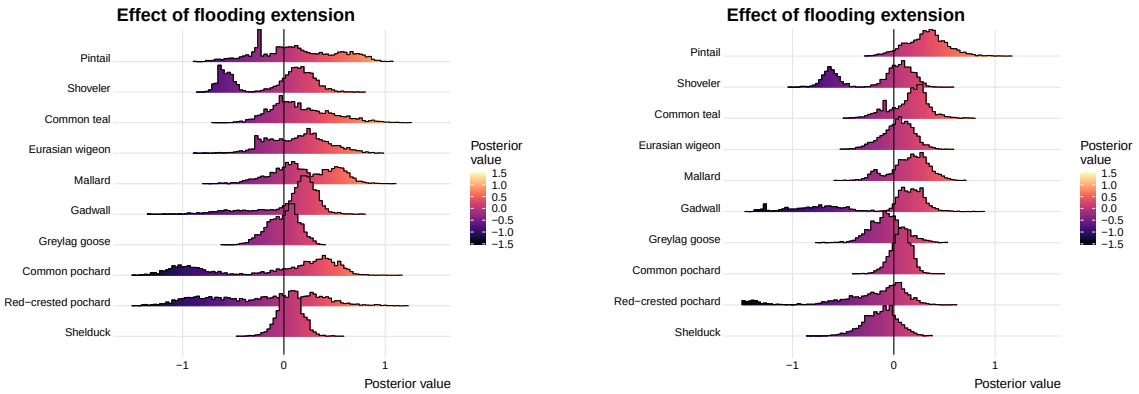

(a) **Before** the Pinatubo eruption (b) **After** the Pinatubo eruption

Figure S2: Posterior distribution for the impact of flooding extension on the population dynamics of each waterfowl species wintering in Doñana wetlands before (A) and after (B) the Mt. Pinatubo eruption.

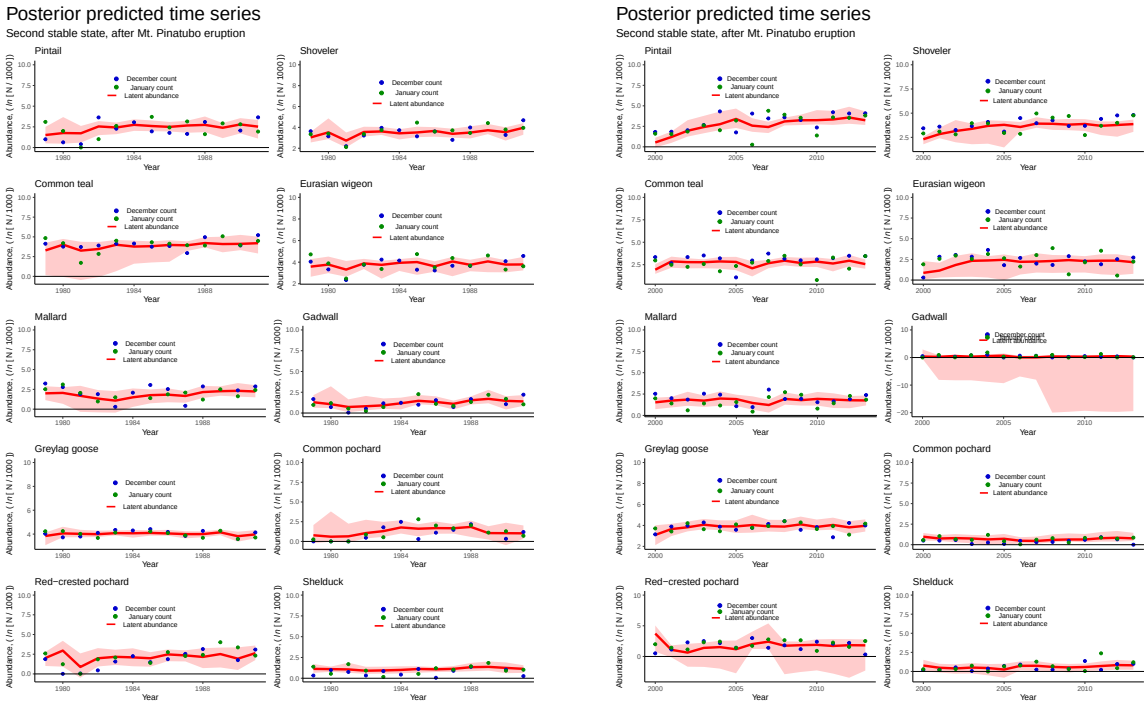

(a) **Before** the Pinatubo eruption (b) **After** the Pinatubo eruption

Figure S3: Posterior predicted datasets testing the ability of the fitted state-space regime-dependent LVR model to replicate the time-series of community abundance before (a) and after (b) the Mt. Pinatubo eruption. For each species and regime, the figures show the observed replicated wintering counts for December (blue dots) and January (green dots), along with the posterior predicted latent abundance (red line) and 95 % Credible Intervals (red shaded region). These distributions were obtained from 1000 replicated time series simulated from the posterior distribution of the parameters of the state-space regime-dependent LVR model.

S4 Stochastic cusp catastrophe modeling

As a theorem for the classification of dynamical systems, catastrophe theory identifies seven canonical, so-called elementary catastrophes (see [14, 15]). Currently, the majority of applications of catastrophe theory in ecology are based on the fold model: a single control parameter induces sudden changes between alternative stable states, separated by unstable parameter regions that induce hysteresis [16, 17]. Here, we used the second canonical catastrophe, the cusp, to test the hypothesis linking planetary-scale perturbations to alternative stable states in the wintering waterfowl community. With an additional control parameter, the cusp catastrophe model considers that some external variables may modulate the behaviour of the bifurcation parameter, inducing discontinuous, nonlinear behavior in a previously smooth, continuous dynamics. Here, we briefly introduce the cusp catastrophe model. Consider a deterministic dynamical system with a state variable $y(t)$, one or several control parameters c, and a potential function of the system, $V(y;c)$:

$$\frac{\partial y}{\partial t} = -\frac{\partial V(y;c)}{\partial y} \tag{S5}$$

where $y, c \in \mathbb{R}$. The minimum of the potential $V(y;c)$ is achieved at equilibrium, $\frac{\partial y}{\partial t} = 0$. Catastrophe theory classifies the behaviour of dynamical systems such as Eqn. S5 in the vicinity of degenerate equilibria (critical points) of the potential $V(y;c)$. An equilibria is degenerate if the higher-order derivatives of the potential function are also 0 at these points. The key is that the degeneracy of the critical points can be unfolded by Taylor-expanding the potential function around them. This set of points can then be classified in seven canonical forms, or universal unfoldings. The second of these canonical forms is the cusp. Interestingly, the cusp catastrophe is structurally stable [18]. Given two control parameters, $\{\alpha, \beta\}$, the canonical form of the potential function for the cusp catastrophe is:

$$-V(y;\alpha,\beta) = -\frac{1}{4}y^4 + \frac{1}{2}\beta y^2 + \alpha y \tag{S6}$$

The equilibrium of the cusp unfolding, as a function of α and β, is thus $\frac{\partial y}{\partial t} = -\frac{\partial V(y;\alpha,\beta)}{\partial y} = 0$, which takes the form:

$$\frac{\partial y}{\partial t} = \alpha + \beta y - y^3 = 0 \tag{S7}$$

The equilibrium points of the cusp catastrophe are the solutions of Eq. S7. There is a range of solutions that the cusp can take, depending on the Cardan's discriminant: $\delta = 27\alpha - 4\beta^3$. If $\delta > 0$, the system has only one solution. But if $\delta < 0$, there are three solutions of the system defined by S7. The set of values of α and β for which $\delta = 0$ is, indeed, the bifurcation set. It is in this region were the system exhibits alternative stable states (see [14, 18–20] for further details). Cobb & Watson [21] provided a stochastic

Table S1: Average parameter values, along with the 95 % confidence interval for the stochastic cusp catastrophe model (see the accompanying paper) fitted through Maximum-Likelihood to the wintering waterfowl community of Doñana marshes. F= flooding extension (ln-Has.); $SAOD$= Stratospheric Aerosol Optical Depth (adim.); x_1= Major dynamic factor, or community trend from the DFA (ln-abundance).

Parameter	**Average**	**95 CI**
$\alpha_1 F$	-0.104	(-0.269, 0.062)
β_0	4.704	(3.645, 5.763)
$\beta_1 SAOD$	-1.119	(-1.740, -0.498)
ω_0	-0.396	(-0.522, -0.271)
$\omega_1 x_1$	4.658	(4.139, 5.180)

approach to the cusp catastrophe. Adding to Eqn. S5 a Wiener (white noise) process $dW(t)$, we get the stochastic version of Eqn. S7:

$$dY = \frac{\partial V(Y;\alpha,\beta)}{\partial Y}dt + dW(t) \tag{S8}$$

which, for the case of the cusp, can be time-indexed and rewritten as

$$dY_t = (-Y(t)^3 + \beta Y(t) + \alpha)dt + \sigma_y dW(t) \tag{S9}$$

where the term within brackets, $-Y(t)^3 + \beta Y(t) + \alpha$, is the drift term and σ_y is the diffusion parameter (variance). The solution of Eqn. S9 satisfies the Fokker–Planck equation [22]. While not solvable analytically, there is an associated stationary density function, $\pi(y)$, that can be easily solved. Given a constant ϕ, this density has the form:

$$\pi(y) = \phi \exp\left\{\frac{2}{\sigma_y^2}\left(-\frac{1}{4}y^4 + \frac{1}{2}\beta y^2 + \alpha y\right)\right\} \tag{S10}$$

The model in S10 reduces to a maximum-likelihood problem if data for fitting α, β and Y is available (see [20, 23] for details). In the accompanying paper we fit the stochastic cusp catastrophe model to the wintering waterfowl community time series of Doñana wetlands using the `R` package `cusp` [20]. Specifically, the empirical model is:

$$\begin{aligned} \alpha &= \alpha_1 F \\ \beta &= \beta_0 + \beta_1 SAOD \\ y &= \omega_0 + \omega_1 x_1 \end{aligned} \tag{S11}$$

where α and β are the asymmetry and bifurcation parameters, respectively [20]. These variables are smooth transformations of the control variables F (flooding extension) and

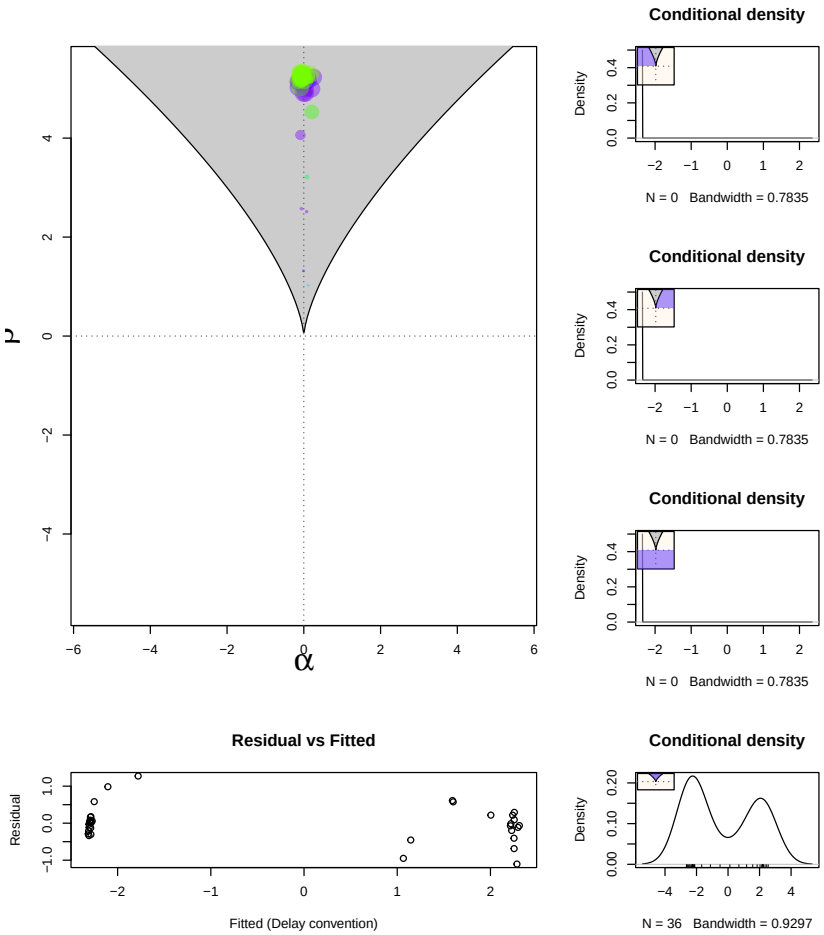

Figure S4: Diagnostic plot for the fitted stochastic cusp catastrophe model (Eqn. S11). The shaded region in the $\alpha - \beta$ plane is the bifurcation set of the cusp catastrophe: the set of points for which the Cardan's discriminant is 0. The crossing of the dotted lines, were $\alpha = \beta = 0$, is the cusp (tipping) point. The conditional density plots show the relative distribution of observed values that are located in each region of the plane. Green dots are above the folded region of the 3D cusp, purple dots are below the folded region.

SAOD (stratospheric aerosol optical depth). The canonical variable y is the state of the system, represented by the major community trend detected by the DFA, x_1. The fitted Maximum-likelihood parameter values of the stochastic cusp catastrophe model in Eqn. S11 are shown in Table S1. The diagnostic plot for the fitted stochastic cusp catastrophe model is shown in Figure S4.

References

1. McCann, K., Hastings, A. & Huxel, G. R. Weak trophic interactions and the balance of nature. *Nature* **395,** 794–798. doi:10.1038/27427 (1998).

2. Berlow, E. L. Strong effects of weak interactions in ecological communities. *Nature* **398,** 330–334. doi:10.1038/18672 (1999).

3. Neutel, A.-m., Heesterbeek, J. A. P. & Ruiter, P. C. D. Stability in Real Food Webs : Weak Links in Long Loops. *Science* **296,** 1120–1123. doi:10.1126/science.1068326 (2008).
4. Mutshinda, C. M., O'Hara, R. B. & Woiwod, I. P. What drives community dynamics? *Proceedings of the Royal Society B: Biological Sciences* **276,** 2923–2929. doi:10.1098/rspb.2009.0523 (2009).
5. Barabás, G., J. Michalska-Smith, M. & Allesina, S. The Effect of Intra- and Interspecific Competition on Coexistence in Multispecies Communities. *The American Naturalist* **188,** E1–E12. doi:10.1086/686901 (2016).
6. Wootton, K. L. & Stouffer, D. B. Many weak interactions and few strong; food-web feasibility depends on the combination of the strength of species' interactions and their correct arrangement. *Theoretical Ecology* **9,** 185–195. doi:10.1007/s12080-015-0279-3 (2016).
7. Downing, A. L. *et al.* Temporal stability vs. community matrix measures of stability and the role of weak interactions. *Ecology Letters* **23,** 1468–1478. doi:10.1111/ele.13538 (2020).
8. Gellner, G., McCann, K. & Hastings, A. Stable diverse food webs become more common when interactions are more biologically constrained. *Proceedings of the National Academy of Sciences* **120,** 2017. doi:10.1073/pnas.2212061120 (2023).
9. Almaraz, P. & Oro, D. Size-mediated non-trophic interactions and stochastic predation drive assembly and dynamics in a seabird community. *Ecology* **92,** 1948–1958. doi:10.1890/11-0181.1 (2011).
10. Almaraz, P., Green, A. J., Aguilera, E., Rendón, M. A. & Bustamante, J. Estimating partial observability and nonlinear climate effects on stochastic community dynamics of migratory waterfowl. *Journal of Animal Ecology* **81,** 1113–1125. doi:10.1111/j.1365-2656.2012.01972.x (2012).
11. Mutshinda, C. M., O'Hara, R. B. & Woiwod, I. P. A multispecies perspective on ecological impacts of climatic forcing. *Journal of Animal Ecology* **80,** 101–107. doi:10.1111/j.1365-2656.2010.01743.x (2011).
12. George, E. I. & McCulloch, R. E. Variable Selection via Gibbs Sampling. *Journal of the American Statistical Association* **88,** 881–889. doi:10.1080/01621459.1993.10476353 (1993).
13. Ishwaran, H. & Rao, J. S. Spike and slab variable selection: Frequentist and Bayesian strategies. *The Annals of Statistics* **33,** 730–773. doi:10.1214/009053604000001147 (2005).
14. Thom, R. Structural stability and morphogenesis (W. A. Benjamin, Inc., Reading, USA, 1975).
15. Arnold, V. I. Dynamical Systems V. Bifurcation Theory and Catastrophe Theory (Springer-Verlag, Berlin, 1994).
16. Dakos, V. *et al.* Ecosystem tipping points in an evolving world. *Nature Ecology & Evolution* **3,** 355–362. doi:10.1038/s41559-019-0797-2 (2019).
17. Scheffer, M. Critical Transitions in Nature and Society (Princeton University Press, Princeton, NJ., 2009).
18. Poston, T. & Stewart, I. Catastrophe Theory and Its Applications (Pitman Publishing, London, UK., 1979).

144 19. Casti, J. Connectivity, Complexity, and Catastrophe in Large-Scale Systems (John Wiley &
145 Sons, Inc., New York, NY, 1979).

146 20. Grasman, R. P. P. P., Maas, H. L. J. v. d. & Wagenmakers, E.-J. Fitting the Cusp Catastrophe
147 in R : A cusp Package Primer. *Journal of Statistical Software* **32.** doi:10.18637/jss.v032.i08
148 (2009).

149 21. Cobb, L. & Watson, B. Statistical catastrophe theory: An overview. *Mathematical Modelling*
150 **1,** 311–317. doi:10.1016/0270-0255(80)90041-X (1980).

151 22. Zeeman, E. C. Stability of dynamical systems. *Nonlinearity* **1,** 115–155. doi:10.1088/0951-
152 7715/1/1/005 (1988).

153 23. Cobb, L. & Zacks, S. Applications of Catastrophe Theory for Statistical Modeling in the
154 Biosciences. *Journal of the American Statistical Association* **80,** 793–802. doi:10.1080/01621459.
155 1985.10478184 (1985).